High temperature gradient wall shear stress micro-sensors for flow separation control

Cécile Ghouila-Houri, Romain Viard, Quentin Gallas, Eric Garnier, Abdelkrim Talbi, Philippe Pernod

High temperature gradient wall shear stress micro-sensors for flow separation control

C. Ghouila-Houri,[1]
Univ. Lille, CNRS, Centrale Lille, ISEN, Univ. Valenciennes, UMR 8520 – IEMN, LIA LICS, Lille, 59000, France
DAAA, ONERA The French Aerospace Lab, Lille, 59014, France
Univ. Lille, CNRS, ONERA, Arts et Metiers Paris Tech, Centrale Lille, Laboratoire de Mecanique des Fluides de Lille – Kampé de Fériet, F-59000, Lille, France

R. Viard.[2]
Fluiditech, Thurmelec, Pulversheim, 68840, France

Q. Gallas,[3]
DAAA, ONERA The French Aerospace Lab, Lille, 59014, France
Univ. Lille, CNRS, ONERA, Arts et Metiers Paris Tech, Centrale Lille, Laboratoire de Mecanique des Fluides de Lille – Kampé de Fériet, F-59000, Lille, France

E. Garnier,[4]
DAAA, ONERA, Université Paris Saclay, F- 92190 Meudon, France

A. Talbi,[5] P. Pernod,[6]
Univ. Lille, CNRS, Centrale Lille, ISEN, Univ. Valenciennes, UMR 8520 – IEMN, LIA LICS, Lille, 59000, France

This paper reports CMOS-compatible calorimetric micro-sensors enabling the bidirectional measurement of wall shear stress in aerodynamic flows. Measuring both the amplitude and the sign of the wall shear stress at small length-scale and high frequencies, the micro-sensors are particularly suitable for flow separation detection and flow control. Their design is hot-wire like with three parallel micro wires suspended over a micro-cavity and mechanically supported using periodic perpendicular micro-bridges. The micro-sensors were manufactured using microelectronics techniques. Implemented on a flexible packaging, the micro-sensors were calibrated in static and in dynamic, in flat plate configuration, inside a turbulent boundary layer wind tunnel. After calibration, twelve micro-sensors have been implemented in a flap model for active flow control experiments. The work included the design and manufacturing of appropriate miniaturized electronics. The micro-sensors successfully detected the natural flow separation. The efficiency of the active flow control for avoiding separation or reattaching a separated flow was also evaluated in this configuration using the micro-sensors.

I. Nomenclature

x	=	position of the micro-sensor
c	=	cord of the flap model
τ	=	wall shear stress
U_∞	=	flow velocity in the center of the wind tunnel test section

[1] PhD Student, DAAA ONERA Lille and LMFL and IEMN.
[2] Research Engineer, Fluiditech Thurmelec.
[3] Research Engineer, DAAA ONERA Lille and LMFL.
[4] Research Engineer, DAAA ONERA Meudon.
[5] Assistant Professor, IEMN, Centrale Lille.
[6] Professor, IEMN, Centrale Lille.

II. Introduction

ONE of the main objectives in research on future vehicles concerns the reduction of fuel consumption and CO_2 or toxic NO_x gases emission. A solution consists in improving the vehicles aerodynamic performances by the mean of flow control. MacMynowski and Williams [1] define flow control as a modification of the natural state of the flow to a wanted state. Lord *et al* [2] consider that this is a small-scale perturbation for a large-scale effect. All in all, it consists in manipulating free stream or wall bounded flows, using active or passive devices, in order to produce favourable changes in the flow such as preventing separation, delaying laminar-turbulent transition, reducing noise, enhancing mixing... Flow control is thereby a technical solution for both safety and ecology issues.

Boundary layer separation is a fluidic phenomenon concerned by flow control. It is a mostly unwanted phenomenon for many technical applications such as automotive industry, and even dangerous in aeronautics. Indeed, separation occurring over flaps is responsible for large performance losses especially during take-off as it simultaneously drastically increases drag and reduces lift [3, 4]. Passive and active devices have been manufactured to encounter this phenomenon but only active closed-loop control enables to adapt the control to the configuration (take-off, landing and cruise are three different configurations for an airplane) and external perturbations (cross-wind, vehicle overtaking…). Indeed, closed-loop control considers electrically commanded actuators for manipulating the flow, and a set of sensors indicating the state of the flow [3].

In flow separation, the wall shear stress plays a key role: the point of separation is characterized by a shear stress null at the wall and in the recirculation area it stress is negative (change of flow direction). Therefore, accurate time-resolved wall shear stress measurement is crucial for implementing a closed-loop control. Flows at moderate Reynolds numbers exhibits typical length scales of 100 µm at the wall or less and time-scales require several kilohertz of bandwidth [5]. Micro-electro-mechanical systems are thereby a technical solution to resolve turbulent flows. Micromachined wall shear stress sensors are usually divided into two groups depending on their measurement techniques: direct techniques using floating element devices [6–8] and indirect techniques such as thermal anemometry [5, 9–12]. Löfdahl and Gad-El-Hak [13] and Sheplak *et al* [14] present reviews on MEMS based shear stress sensor and discuss the advantages and drawbacks of each techniques.

In this paper is reported a micromachined wall shear stress micro-sensor based on both thermal anemometry and calorimetric principle and enabling the bidirectional measurement of wall shear stress in aerodynamic flows. In the first part of the paper, the design and fabrication of the micro-sensors are presented, along with calibrations in a turbulent boundary layer wind tunnel. Then, a second part presents the implementation of twelve micro-sensors in a flap model along with miniaturized electronics. A large wind tunnel allowed to perform flow control experiments on this model and the first results are presented and discussed in the final part of the paper.

III. The micro-sensor design, fabrication and calibration

A. Fabrication and characterization in cleanroom

The micro-sensors at stake in this paper are based on both thermal anemometry and calorimetric principle. They are indeed composed of an electrically heated micro-wire, called a heater, and two cold-wires placed on both sides. The central wire is devoted to the measure of wall shear stress using thermal anemometry meaning that the heat losses between the hot-wire and the fluid due to forced convection gives an image of the flow velocity near the wall. Designed as identical in dimensions and materials, the two lateral wires are symmetrically heated by the central hot-wire. The flow direction will break the thermal boundary layer symmetry and the upstream lateral wire will be more cooled than the downstream one (Fig. 1). This principle is called calorimetric. Coupling both principles, the micro-sensors are able to detect the wall shear stress amplitude and sign. This property gives a direct advantage for flow separation detection, as separation is characterized by both a diminution of the wall shear stress amplitude and an inversion of its sign.

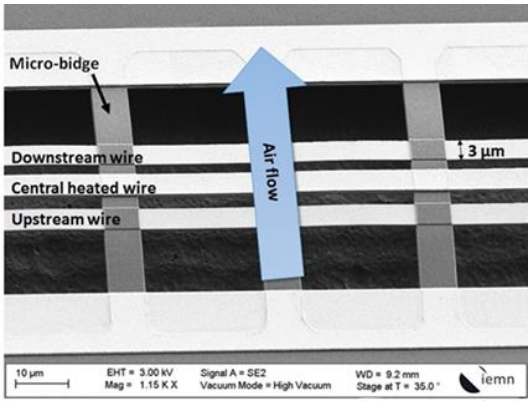

Fig. 1 Scanning Electron Microscopy image of the sensitive part of the micro-sensor.

The micro-sensors sensitive part is then composed of three parallel wires whose dimensions are 1 mm long, three µm wide and less than 1 µm thick. The lateral wires are composed of a SiO_2 layer for mechanical support and Ni/Pt multilayer forming the metallic measurement wire. The central hot-wire is engineered with multiple layers including SiO2, Ni/Pt multilayer, another layer of SiO_2 and Au layer. The heating current cross the Au layer and the Ni/Pt multilayer is used for measurement. Contrary to conventional hot-wire sensors [9, 10]; this microstructure uncouples heating and measure in electronics [15].

The wires are free from the substrate, suspended over a 20 µm deep cavity. Suspended periodic perpendicular micro-bridges are disposed along the wire for mechanical support (Fig. 1).

The fabrication process includes seven CMOS-compatible main steps (CMOS for Complementary Metal Oxide Semiconductor) and needs four photolithography masks. The different steps leading to the 140 micro-sensors manufactured on a 3 in. wafer (Fig. 2 (a)) are presented in details in [16]. Electrical and thermal characterizations have been performed on each micro-sensors leading to a measured TCR (Temperature Coefficient of Resistance) of 2380 ppm/°C and a heating elevation of 9°C/mW for the central wire and 5 °C/mW for the lateral wires [15]. Thermal imaging presented in Fig. 2 (b) demonstrates the efficiency of thermal insulation as the heating located in the wires and there are few heat losses into the micro-bridges.

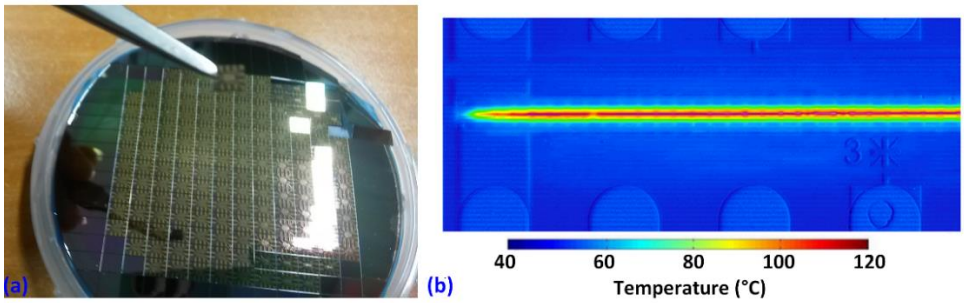

Fig. 2 (a) 3 in. wafer with 140 micro-sensors (b) Thermal imaging of the sensors supplied with 10 mW heating power.

B. Calibration in wind tunnel

After design, fabrication and characterizations, the micro-devices were calibrated in a turbulent boundary layer wind tunnel. The test section is 30 cm x 30 cm and the wind velocity goes up to about 40 m/s.

The boundary layer was characterized using a hot-wire probe mounted on a motorized support (Fig. 3). These measurements enables to deduce the momentum thickness and the skin friction coefficient using Coles-Fernholz equation [17] and finally the experimental wall shear stress [15]. For upstream U_∞ velocities reaching 40 m/s, the corresponding shear stress reach up to 2.5 Pa.

The micro-sensor is designed for flow control meaning that its purpose is to resolve shear stress going from -0.2 (separated flow) to 40 Pa (near jets). In practice, the wind tunnel enables to calibrate the sensor up to 2.5 pa.

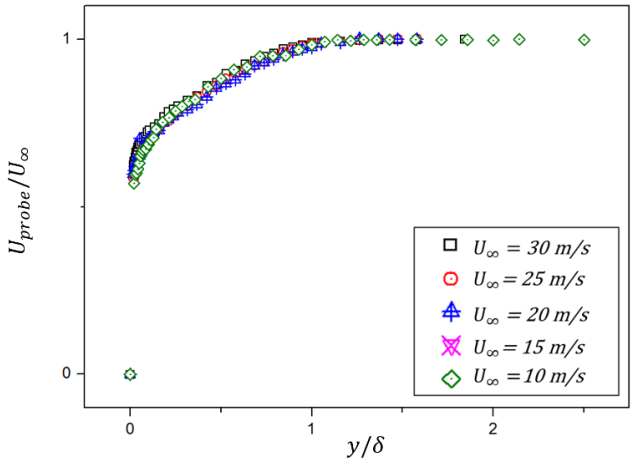

Fig. 3 Boundary layer characterization using a hot-wire probe on a motorized support

The micro-sensors are designed keeping robustness as an important parameter for they can measure real in flight with flow control shear stress. On one hand, shear stress on airplanes can reach a few Pascal, but introducing active flow control, it can reach up to several dozens of Pascal, near the actuation system. The micro-sensors are designed to support and accurately measure such shear stress however the wind tunnel used for calibration only reach up to 2.5 Pa meaning that future work on high shear stress values is needed.

The micro-sensors work in constant temperature (CT) mode meaning that the central wire temperature is maintained constant by adapting the heating current crossing the Au layer in closed-loop control. The wire temperature is measured using the Ni/Pt multilayer resistance.
The micro-sensors were mounted on the wind tunnel wall for calibration presented in Fig. 4. A flexible packaging enables to recover contacts using surface mounted component welding technique.
Figure 4 (a) presents the central wire response to the wall shear stress amplitude variation. The micro-sensor response fits a polynomial like conventional thermal wall shear stress sensors [5]. Figure 4 (b) present the sensitivity of the lateral wires to the flow direction. For this experiment, the difference of resistance between the lateral wires is measured as an image of the difference of temperature (via the TCR).

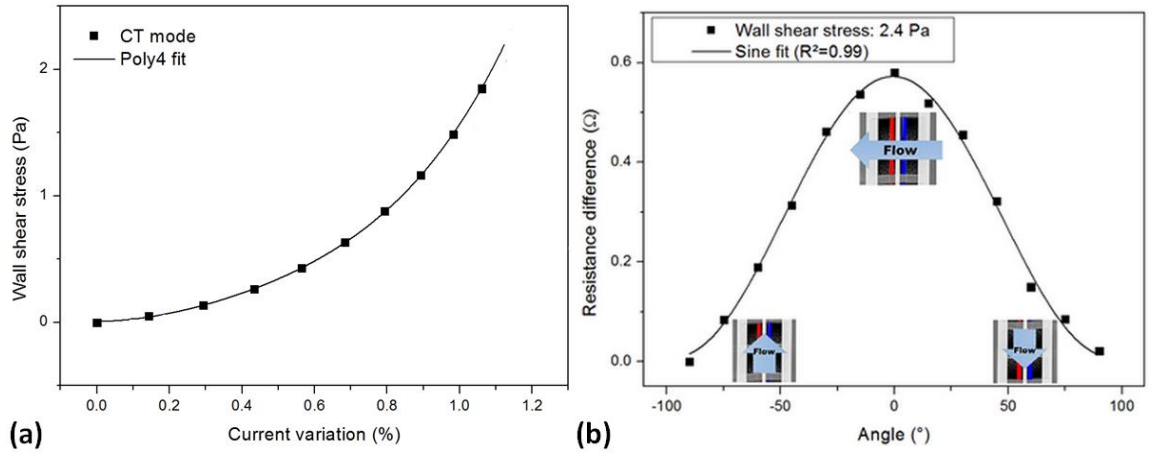

Fig. 4 (a) Central wire calibration in constant temperature mode (b) Difference of lateral resistances versus flow direction for $\tau = 2.4$ Pa.

The micro-sensor was also characterized dynamically at high velocity in Fig. 5. This figure presents the power spectral density measured for $U_\infty = 38\ m/s$. The response is relatively flat up to 1 kHz and starts to decrease as the boundary layer losses energy. In this experiment however the impact of the cavity of flexible packaging appears. Indeed, as contacts are front-side, the sensor is a bit under the wall. The signal is then damped for low frequencies as the cavity slightly filters it.

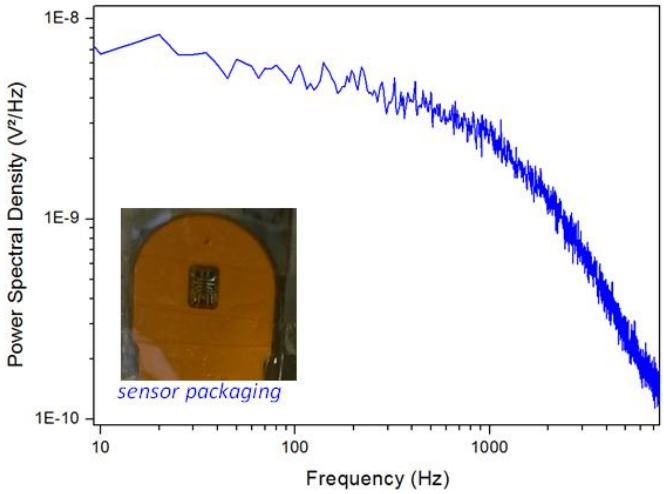

Fig. 5 Power Spectral Density of the micro-sensors at $U_\infty = 38\ m/s$

IV. Implementation of an array of micro-sensors in a flap model with miniaturized electronics

The two following parts are dedicated to flow control experiments on a flap model. Flaps are used on airplanes (Fig. 6 (a)) to delay separation during take-off and landing.
The flow control experiments planed using the micro-sensors follow the work of Chabert *et al* [18]. This work studies the natural flow separation on an inclined flap using tomoscopy flow visualizations and hot-film sensors measurements. Open loop control using Festo® MHE2 valves is also demonstrated. In this work, the same configuration is used but the hot-film sensors along the cord are replaced by the calorimetric micro-sensors (Fig. 6 (b)). The same actuators are used.

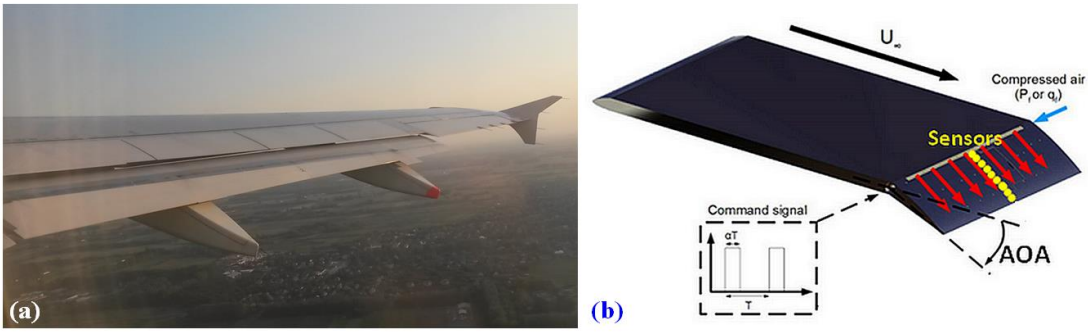

Fig. 6 (a) Flap on A340 (b) Schematic of the experiment with the flap model instrumented with the micro-sensors disposed along the cord.

The experiment take place in the large L1 wind tunnel in ONERA Lille (Fig. 7 (a)). The wind tunnel test section has a diameter of 2.40 m and the length of the working area is about 10 meters. The flap model is placed between two plates to avoid side effects. Therefore, the flow is almost two-dimensional at the center of the flap. A 867 mm long flat plate stabilize the boundary layer before the flap. The flap is unslotted, has $c = 220\ mm$ long chord and is based on NACA 4412 airfoil shape.
As seen on Fig. 7 (b), twelve micro-sensors have been implemented in the flap model with embedded miniaturized electronics designed and manufactured by Fluiditech. Two of them are individual sensors with proper CT electronics and are located close to the leading edge of the flap. A flexible 3 mm thick strip of ten sensors with mutual electronics takes place in the thinner part of the model and reaches up to 30 mm far from the trailing edge. The twelve sensors are flush-mounted in the model and the flexible strip enables to follow the airfoil shape camber.

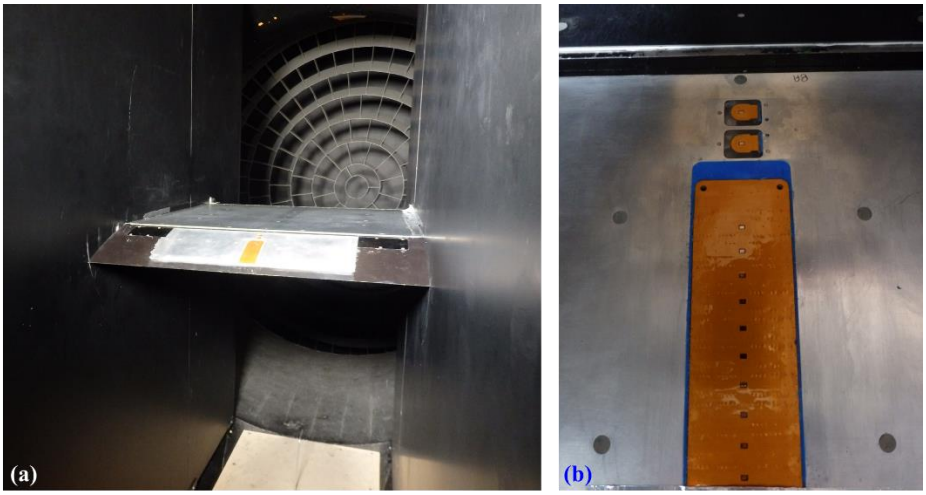

Fig. 7 (a) Flap model with implemented micro-sensors (b) Zoom on the twelve micro-sensors: two individual sensors at the leading edge and a strip of ten sensors with common electronics

Figure 8 shows in (a) a zoom on the leading edge sensors and in (b) their individual miniaturized CT electronics. The micro-sensors electronics is only 3 mm high and 50 mm long. The micro-sensors are flush-mounted at the flap model surface using PMMA support manufactured for following the flap camber. Figure 8 (c) shows the 115 mm long flexible strip with a focus on two micro-sensors. There are 10 micro-sensors embedded into the flexible strip, 8 mm away one from the other. Being flexible and 3 mm thick, the strip matches the flap camber. The small volume is a key parameter for the success of the micro-sensors implementation in the model. Figure 8 (d) shows an instrumentation electronics box. Three are needed: one for each individual sensor and one for the strip. The three boxes present dimensions small enough to be embedded inside the flat plate upstream of the flap.

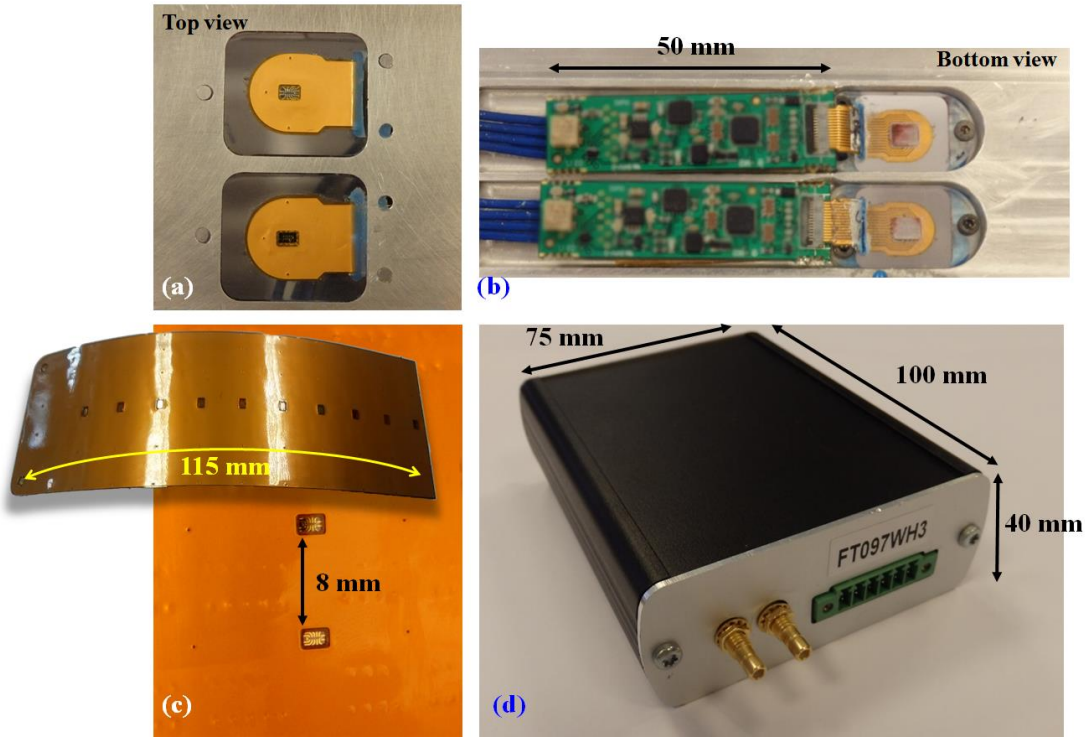

Fig. 8 (a) The two leading edge micro-sensor (b) Individual CT electronics for the leading edge sensors (c) Zoom on three sensors from the strip (d) One of the three instrumentation electronics box embedded inside the flat plate.

V. Flow control experiments

Active flow control experiments were performed using the Festo® MHE2 valves as continuous or pulsed jets actuators and the micro-sensors for measurements. The first results are displayed in Fig. 9, 10 and 11 and deal with the natural separation detection, the control of separation and the control of a separated flow. For these last two point, the control objective differs according to the situation: if the flow is attached the goal will be to avoid or at least delay the separation (control of separation) whereas if the flow is separated the objective will be to reattach it (control of a separated flow).
All the presented results comes from the second individual sensor placed at $x/c = 0.3$, with an upstream velocity $U_\infty = 24.5\ m/s$

In Chabert's work, the flow separation point was deduced by comparing the hot-films responses two by two. Detecting both the amplitude and the flow direction, the micro-sensors developed here do not need such comparison: they can detect the flow separation by their own, independently one from the other. As shown on Fig. 9 in black symbols, the separation at $x/c = 0.3$ occurs for an angle of attack of about 17°: at this angle, the equivalent shear stress is zero and becomes negative for higher angles. The amplitude is measured using the central wire and the sign is deduced from the temperature difference between the two lateral wires.

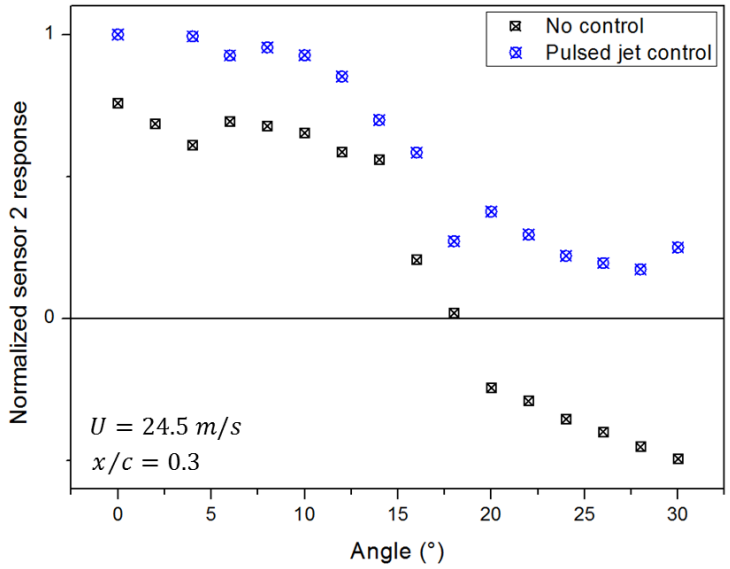

Fig. 9 <u>Control of separation</u>: normalized response of the micro-sensor at $x/c = 0.3$ without control and with pulsed jet control.

The separation is also visible in terms of shear stress fluctuations as shown on Fig. 10 (a): at 2° and 10°, the flow is attached to the flap for $x/c = 0.3$, at 20° the flow has just separated and the fluctuations start to attenuate and finally at 30° the flow is fully separated and the fluctuations are very damped.
Active flow control using pulsed jets allows controlling separation and, at $x/c = 0.3$ for this example, the control succeed in avoiding separation. Indeed as shown on Fig. 9 with blue symbols, the flow direction does not change after 17° of angle meaning that the shear stress remains positive. The control has also a direct effect on the shear stress fluctuations (Fig. 10 (b)) that reach the same level as at natural attached flow at 2°. A set of peaks appear due to the pulsed actuation. The main peak is at 60 Hz and corresponds to the pulsed jet frequency. The jets are indeed working at 60 Hz with 50% duty cycle and supplied by 20 g/s of airflow.

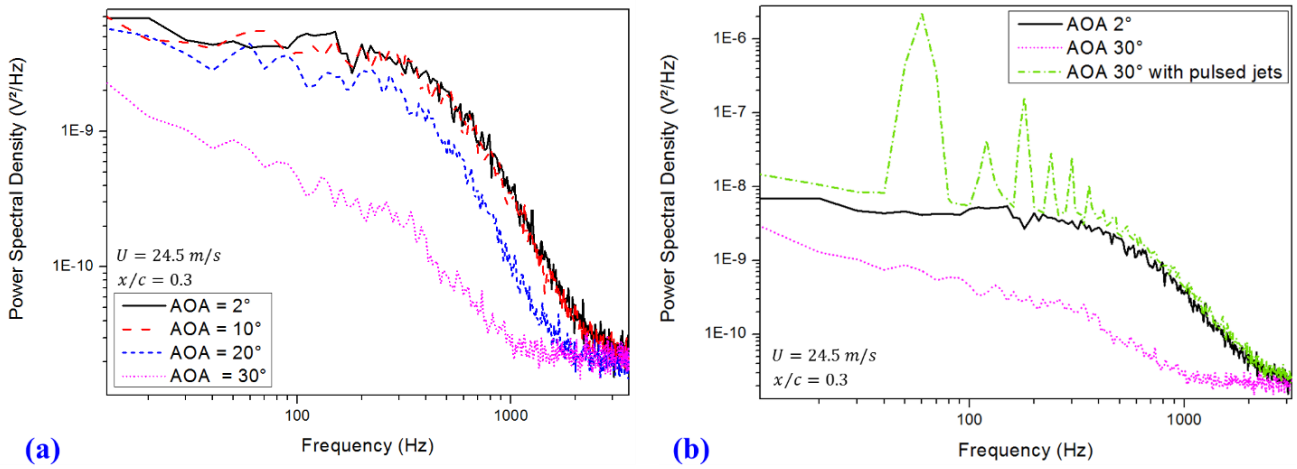

Fig. 10 (a) <u>Natural separation</u>: PSD at different angles of attack without control; (b) <u>Control of separation</u>: PSD at 2° (attached) 30° (separated) and 30° with pulsed jets.

Figure 11 (a) presents the control of a separated flow. At 24° of angle of attack, the flow is naturally fully separated, and the shear stress amplitude is less important. When turning on the active flow control with either steady blowing or pulsed jets, the shear stress increases. For pulsed jet, the mean amplitude nearly reach the one of the attached flow. For steady blowing, it is even more important. This is explained easily considering the sensor position, which is not far from the actuators and the fact that the jets are supplied with 20 g/s of airflow. Figure 11 (b) shows the separation of the controlled flow when the actuation is turned off.

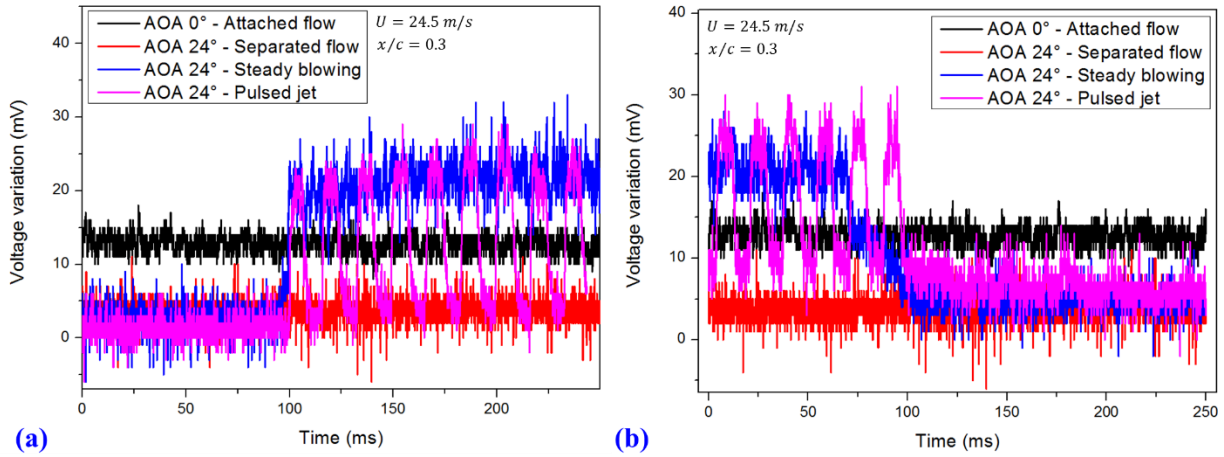

Fig. 11 (a) <u>Control of a separated flow</u>: response of the micro-sensor at $x/c = 0.3$ at 0°, 24° without control, 24° with steady blowing and 24° with pulsed jet control (b) Natural separation after turning off the actuators

VI. Conclusion and future work

This paper presented micromachined wall shear stress sensors based on thermal transduction and calorimetric principle and designed for flow control applications in aeronautics. The main advantages of the micro-sensors compared to conventional sensors lie in the miniaturized dimensions, the integration capability for implementation in models and the simultaneous measurement of the wall shear stress amplitude and sign. The first part of the paper presented the

unconventional design of the micro-sensors along with the calibration in wind tunnel. The second and third part of the paper were devoted to the implementation of twelve micro-sensors with miniaturized electronics into a flap model and the active flow control experiments run in open loop configuration. The success of implementation is the first point to highlight. The second point is that the micro-sensors demonstrated their ability to detect the natural flow separation and the effect of the active control. Control of separation and control of a separated flow have both been tested and performed.

In future work, we are currently working on improving the electronics to enlarge the bandwidth up to several dozens of kilohertz. We also develop a new packaging to improve the signal to noise ratio and avoid damping signal. All these improvements are part of the development of sensors maturity in order to characterize the micro-sensors in other flow configurations.

VII. Acknowledgments

The French National Research Agency (ANR) in the framework of the ANR ASTRID "CAMELOTT" Project funded this work. It was supported by the regional platform CONTRAERO in the framework of the CPER ELSAT 2020 Project. The ELSAT 2020 project is co-financed by the European Union with the European Regional Development Fund, by the French State and the Hauts de France Region under the State Region Contracts (CPER). The authors also thank RENATECH, the French national nanofabrication network, and the ONERA Specific Devices and Models unit, which provided the design and fabrication of the test model for the micro-sensors implementation.

VIII. References

[1] MacMynowski, D. G.; Williams, D. Flow Control Terminology. In *Fundamentals and Applications of Modern Flow Control*; American Institute of Aeronautics and Astronautics; pp. 59–71 ISBN 978-1-56347-983-0, 2009.

[2] Lord, W.; MacMartin, D.; Tillman, G. Flow control opportunities in gas turbine engines. In *Fluids 2000 Conference and Exhibit*; American Institute of Aeronautics and Astronautics, 2000.

[3] Gad-el-Hak Flow Control: The Future. *J. Aircr.*, *38*, 402–418, 2001

[4] Gad-el-Hak, M.; Bushnell, D. M. Separation Control: Review. *J. Fluids Eng.*, *113*, 5–30, 1991, doi:10.1115/1.2926497.

[5] Sheplak, M.; Chandrasekaran, V.; Cain, A.; Nishida, T.; Cattafesta III, L. N. Characterization of a silicon-micromachined thermal shear-stress sensor. *AIAA J. 40*, 1099–1104, 2002.

[6] Schmidt, M. A.; Howe, R. T.; Senturia, S. D.; Haritonidis, J. H. Design and calibration of a microfabricated floating-element shear-stress sensor. *IEEE Trans. Electron Devices*, *35*, 750–757, 1988, doi:10.1109/16.2527.

[7] Chandrasekharan, V.; Sells, J.; Arnold, D. P.; Sheplak, M. Characterization of a MEMS-based floating element shear stress sensor. In *47th AIAA Aerospace Sciences Meeting including the New Horizons Forum and Aerospace Exposition*; 2009.

[8] Lv, H.; Jiang, C.; Xiang, Z.; Ma, B.; Deng, J.; Yuan, W. Design of a micro floating element shear stress sensor. *Flow Meas. Instrum.*, *30*, 66–74, 2013, doi:10.1016/j.flowmeasinst.2012.11.004.

[9] Bailey, S. C. C.; Kunkel, G. J.; Hultmark, M.; Vallikivi, M.; Hill, J. P.; Meyer, K. A.; Tsay, C.; Arnold, C. B.; Smits, A. J. Turbulence measurements using a nanoscale thermal anemometry probe. *J. Fluid Mech. 663*, 160–179, 2010, doi:10.1017/S0022112010003447.

[10] Talbi, A.; Gimeno, L.; Gerbedoen, J.-C.; Viard, R.; Soltani, A.; Mortet, V.; Preobrazhensky, V.; Merlen, A.; Pernod, P. A micro-scale hot wire anemometer based on low stress (Ni/W) multi-layers deposited on nano-crystalline diamond for air flow sensing. *J. Micromechanics Microengineering 25*, 125029, 2015, doi:10.1088/0960-1317/25/12/125029.

[11] Jiang, F.; Lee, G.-B.; Tai, Y.-C.; Ho, C.-M. A flexible micromachine-based shear-stress sensor array and its application to separation-point detection. *Sens. Actuators Phys. 79*, 194–203, 2000, doi:10.1016/S0924-4247(99)00277-0.

[12] Xu, Y.; Tai, Y.-C.; Huang, A.; Ho, C.-M. IC-integrated flexible shear-stress sensor skin. *J. Microelectromechanical Syst. 12*, 740–747, 2003, doi:10.1109/JMEMS.2003.815831.

[13] Löfdahl, L.; Gad-el-Hak, M. MEMS-based pressure and shear stress sensors for turbulent flows. *Meas. Sci. Technol.*, *10*, 665, 1999.

[14] Sheplak, M.; Cattafesta, L.; Nishida, T.; McGinley, C. B. MEMS shear stress sensors: promise and progress. In *24th AIAAA aerodynamic measurement technology testing conference. Florida Univ Gainesville mechanical and aerospace engineering*; 2004.
[15] Ghouila-Houri, C.; Gallas, Q.; Garnier, E.; Merlen, A.; Viard, R.; Talbi, A.; Pernod, P. High temperature gradient calorimetric wall shear stress micro-sensor for flow separation detection. *Sens. Actuators Phys. 266*, 232–241, 2017, doi:10.1016/j.sna.2017.09.030.
[16] Ghouila-Houri, C.; Claudel, J.; Gerbedoen, J.-C.; Gallas, Q.; Garnier, E.; Merlen, A.; Viard, R.; Talbi, A.; Pernod, P. High temperature gradient micro-sensor for wall shear stress and flow direction measurements. *Appl. Phys. Lett. 109*, 241905, 2016, doi:10.1063/1.4972402.
[17] Nagib, H.; Chauchan, K. A.; Monkewitz, P. A. Approach to an asymptotic state for zero pressure gradient turbulent boundary layers. *Philos. Trans. R. Soc.*, *365*, 755–770, 2007.
[18] Chabert, T.; Dandois, J.; Garnier, E.; Jacquin, L. Experimental detection of a periodically forced turbulent boundary layer separation. *Exp. Fluids 54*, 2013, doi:10.1007/s00348-012-1430-1.